



THEORETICAL STUDY OF THE ELECTRONIC SPECTRA, STATIC FIRST HYPERPOLARIZABILITY AND ANTIRADICAL CAPACITY OF 2-PYRIDONE TAUTOMERS BY DENSITY FUNCTIONAL THEORY (DFT)

C. LAXMIKANTH
Department of Physics, The
University of Dodoma, Dodoma,
Tanzania
dr.cherupally@gmail.com

N. SURENDRA BABUAND
Department of Chemistry, The
University of Dodoma, Dodoma,
Tanzania
nsbabusk@gmail.com

ISAAC ONOKA
Department of Chemistry, The
University of Dodoma,
Dodoma, Tanzania

ABSTRACT

The geometries, electronic structures, polarizabilities and hyperpolarizabilities of 2-Pyridone tautomers were studied based on Density Functional Theory (DFT) using the hybrid functional B3LYP. Here we explore in the Density Functional Theory (DFT) framework the antiradical activity of 2-pyridone. Using the single charge transfer model electrodonating (ω^-) and electro accepting (ω^+) powers, a Donor Acceptor Map (DAM) was employed to classify them as good or bad antiradicals. Ultraviolet-visible (UV-Vis) spectrum was investigated by Time Dependent DFT (TD-DFT). Features of the electronic absorption spectrum in the visible and near-UV regions were assigned based on TDDFT calculations. Polarizability and the first order hyperpolarizability values have been computed theoretically.

Key words: 2-pyridone, antiradical activity, TD-DFT, polarizability and the first order hyperpolarizability

1. INTRODUCTION

The heterocyclic skeleton containing nitrogen atom is the basis of many essential pharmaceuticals and of many physiologically active natural products. Molecules containing heterocyclic substructures continue to be attractive targets for synthesis since they often exhibit diverse and important biological properties. Accordingly, novel strategies for the stereo selective synthesis of hetero polycyclic ring systems continue to receive considerable attention in the field of synthetic organic chemistry. Pyridine-2(1H)-one (2-Pyridone) is colorless crystalline solid is used in peptide synthesis. It is well known to form hydrogen bonded structures somewhat related to the base-pairing mechanism found in RNA and DNA. The most prominent feature of 2-pyridone is the amide group; a nitrogen with a hydrogen bound to it and a keto group next to it. In peptides, amino acids are linked by this pattern, a feature responsible for some remarkable physical and chemical properties.

The density functional theory (DFT) has emerged as a reliable standard tool for the theoretical treatment

of structures as well as electronic and absorption spectra. Its time-dependent extension, called time-dependent DFT (TD-DFT), can give reliable values for the valence excitation energies with standard exchange-correlation functionals. In this study, density functional calculations (DFT) using the B3LYP functional with the 6311++G(d) basis set were performed to predict the orbital energy levels and time dependent DFT (TDDFT) calculations carried out to obtain the electronic absorption spectra of the 2-Pyridone tautomers.

2. COMPUTATIONAL METHODS

All the geometries of the 2-pyridone tautomers (Fig. 1) have been fully optimized using the B3LYP method within the framework of density functional theory (DFT) in conjunction with the 6-311++G(d,p) basis set, i.e., Becke's three parameter non-local hybrid exchange potential with the non-local correlation functional of Lee, Yang, and Parr [1]. All these calculations were carried out on a Pentium V personal computer by means of GAUSSIAN 09 program package [2]. The excitation energies and oscillator strengths for the lowest 6 singlet-singlet transitions at the optimized geometry in the ground state were obtained in TDFT calculations using the same basis set as for the ground state. According to the calculated results, the UV-Vis absorption spectra were simulated by a Gaussian convolution with a full width at half-maximum of 0.4 eV [3].

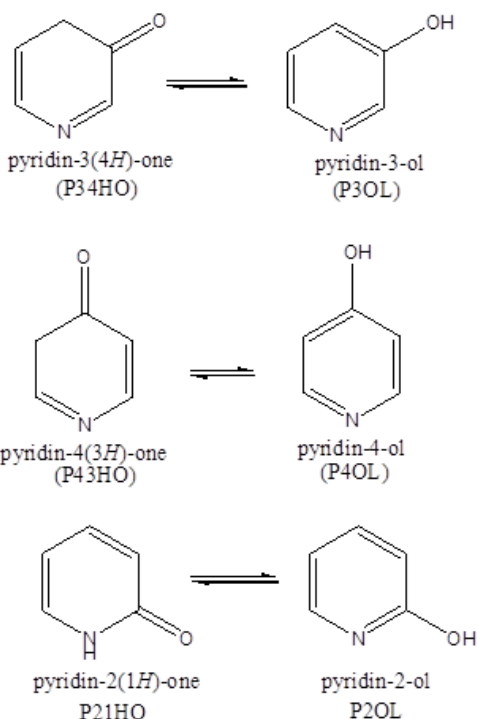


Fig:1. Structures of 2-Pyridone and 2-Pyridinethione tautomers

3. RESULTS AND DISCUSSION

3.1. Antiradical activity

Antiradical activity of a compound may be evaluated from the oxidation and reduction potential that is based in the ionization potential (I) and electron affinity (A), respectively. A molecule with a low value of I is easily oxidizable, therefore, it is good electron donor or good antioxidant. On the other hand, a molecule with high positive values of A is a good electron acceptor or good antireductor. It is known that antioxidant and antireductor properties can be determined by electronic bonding energies (I and A) [4]. Gázquez et al. [5] proposed the electrodonating (ω^-) and electroaccepting power (ω^+) through the analysis of the behavior of a molecule in an idealized medium capable to donate or accept charge. Within this model the electrodonating power is defined as

$$\omega^- = \frac{(3I + A)^2}{16(I + A)} \quad (1)$$

and the electroaccepting power as

$$\omega^+ = \frac{(I + 3A)^2}{16(I + A)} \quad (2)$$

According to the model employed by these authors, the quadratic term in the numerator corresponds to the chemical potential I and the term in the denominator corresponds to the hardness g. In molecules capable to donate charge, ω^- gives more emphasis to I. Contrary, in molecules capable to accept charge; ω^+ gives more emphasis to A.

Martinez et al. [6] proposed to normalize the values of electrodonating (ω^-) and electroaccepting (ω^+) powers through a donor (R_d) and acceptor (R_a) index respectively. Where, R_d is the relationship of ω^- from the chemical species of interest, L, with respect to the ω^- of a well-known electron donor like the Na atom.

$$R_d = \frac{\omega_L^-}{\omega_{Na}^-} \quad (3)$$

and R_a is the relation of ω^+ of L with respect to ω^+ of the F atom, which is a well-known electron acceptor.

$$R_a = \frac{\omega_L^+}{\omega_F^+} \quad (4)$$

Martinez suggested the classification of chemical species like good or bad electron donors or electron acceptors in a Donor–Acceptor Map. The DAM is obtained by the ratio of a donor index R_d /acceptor index R_a , Fig. 2. With the above chart, we can say that from global properties we can evaluate the antiradical behavior of a molecule.

Bad acceptor Bad donor	Good acceptor Bad donor Good antireductor
The worst antiradical	Good antiradical
Bad acceptor Good donor Good antioxidant	Good acceptor Good donor
Good antiradical	The best antiradical

Fig. 2. (“As is”). Donor–Acceptor Map (DAM) [26]

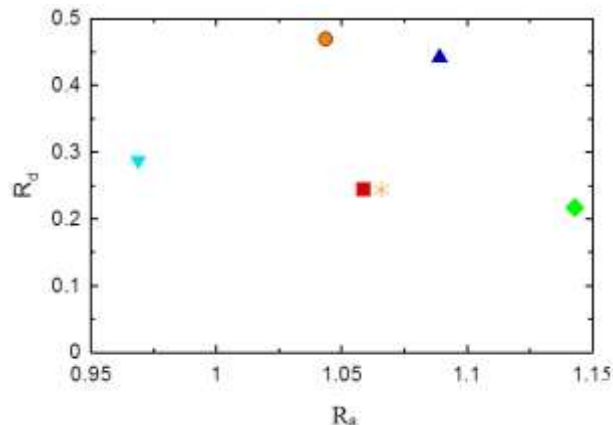
The values of ionization potential(I), electron affinity(A), electrodonating (ω^-), electroaccepting (ω^+) power, donor R_d and acceptor R_a index are shown in Table 2. Ionization potential (I), for P43HO tautomer have high value (7.2799) than its enol form P3OL (6.8244), in the case of P43HO (7.2799) and

its enol form P4OL (7.2720) are approximately same values. But the tautomer P21HO (6.3492) is less than its enol form P2OL (6.8633). The order of good electron donors: P2OL < P21HO < P3OL < P34HO < P4OL < P43HO. For electron affinity (A), the three ketotautomers P34HO, P43HO and P21HO values of 2.9916, 2.7503 and 1.5987 eV respectively, compared with the A values of 1.1652, 0.8392 and 1.1418 eV for their enol tautomers P3OL, P4OL and P2OL, respectively, so that, the enol tautomers are not good electron acceptors.

The donor and acceptor index were calculated from Eqs. (3) and (4). In (3) we can see that, if $R_d = 1$ the ester molecule is as good electron donor as the Na atom. If $R_d > 1$ it is worst electron donor than Na. If $R_d < 1$ it is better electron donor than Na. On the other hand, in (4), if $R_a = 1$ the ester is as good electron acceptor as the F atom. If $R_a > 1$ it is better electron acceptor than F and if $R_a < 1$ it is worst electron acceptor than F [7-9]. R_d versus R_a index were plotted in the DAM. With respect to the electro donating (ω^-) and electro accepting (ω^+) power, low values of ω^- imply good capability to donate an electron and high values of ω^+ imply good capability to accept an electron [5,6]. On Fig. 3 DAM for R_d and R_a values for 2-pyridone tautomers are shown.

Table 1 Values of I, A, ω^- , ω^+ , R_a and R_d

Tautomer	I	A	ω^-	ω^+	R_a	R_d
P34HO	7.0184	2.9916	3.6104	1.5971	1.0435	0.4697
P3OL	6.8244	1.1652	3.6627	0.8331	1.0586	0.2450
P43HO	7.2799	2.7503	3.7678	1.5030	1.0890	0.4421
P4OL	7.2720	0.8392	3.9548	0.7385	1.1430	0.2172
P21HO	6.3492	1.5987	3.3521	0.9768	0.9688	0.2873
P2OL	6.8633	1.1418	3.6872	0.8265	1.0657	0.2431



3.2 Electronic Structures

The molecular orbitals involved in the analyzed transitions were examined by the DFT method. The vertical excitation energy and oscillator strength along with the main excitation configuration are listed in Table I. The major electronic absorption bands are assigned to those excitations with significant oscillator strengths. The HOMO and LUMO orbitals of 2-pyridone tautomers are shown in Fig. 2 as a representation. The electron distribution of the HOMO orbital is delocalized over the π -system with the highest electron density centered on the central oxygen atom. It is noticed that the LUMO orbital has larger compositions of the nitrogen atom compared with the HOMO orbital in case of P43HO tautomer. The absolute energies of the HOMOs and LUMOs are presented in Table 1. The simulated absorption spectra of the 2-pyridone tautomers are shown in Fig. 2. The first optically allowed electronic transition of λ_{max} for P34HO, P3OL, P43HO, P4OL, P21HO and P2OL are predicted to populate the HOMO \rightarrow LUMO transitions at 310.66, 246.90, 277.33, 203.49, 287.63 and 244.75 nm, respectively. The simulated absorption spectra of the six tautomers in gas phase are shown in Fig 4.

Fig. 3. (“As is”). DAM of 2-pyridone tautomers in gas phase

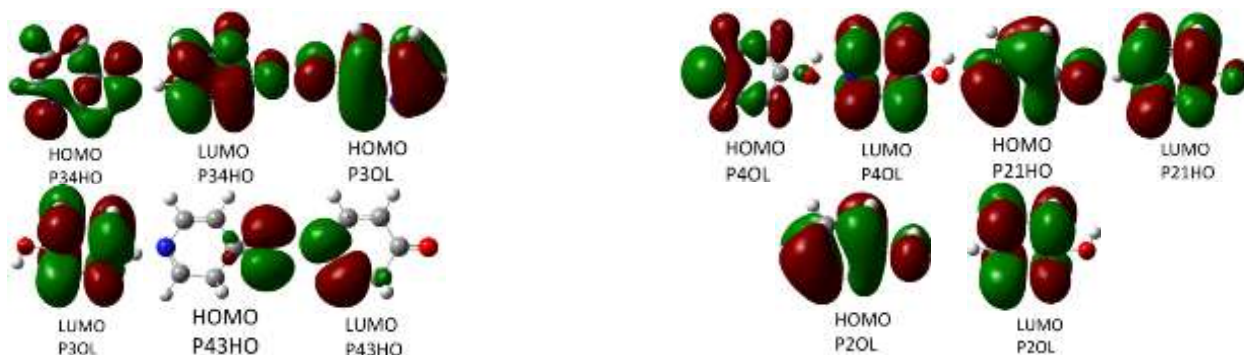
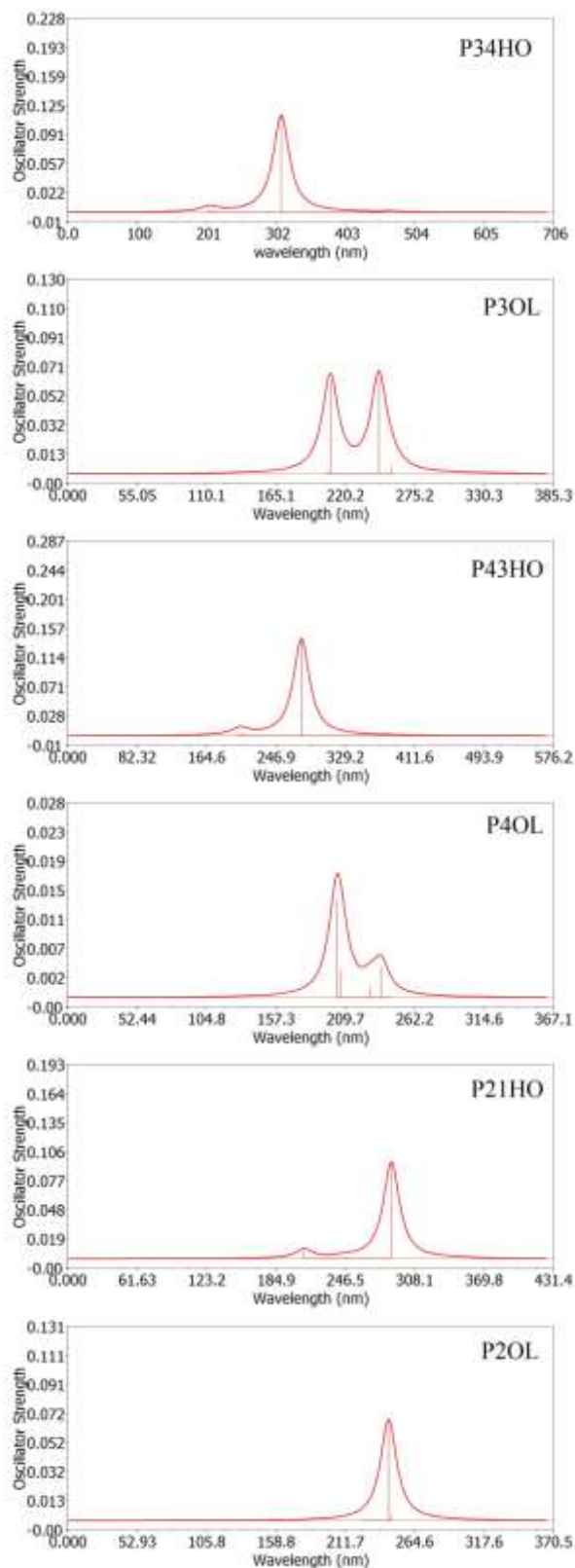


Fig. 4. HOMO and LUMO of the 2-Pyridone and 2-Pyridinethione tautomers computed on the ground-stated geometries

Table. 2. Excitation energy (E and calculated λ), oscillator strength (f) and main configuration of 2-Pyridone tautomers (H = HOMO, L = LUMO, L+1 = LUMO+1, etc.)

Tautomer	E / eV	λ / nm	f	Configuration	Assignment
P34HO	2.6336	470.78	0.0009	H \rightarrow L (+99%)	$\pi \rightarrow \pi^*$
	3.9909	310.66	0.1140	H-1 \rightarrow L (+98%)	
	4.2334	292.87	0.0010	H-2 \rightarrow L (+93%); H \rightarrow L+1 (+6%)	
	5.2344	236.86	0.0000	H \rightarrow L+2 (+6%); H \rightarrow L+1 (+92%)	
	5.8550	211.76	0.0000	H \rightarrow L+2 (+97%)	
	6.1057	203.06	0.0000	H-1 \rightarrow L+2 (+99%)	
P3OL	4.8258	256.92	0.0043	H-1 \rightarrow L (+99%)	$\pi \rightarrow \pi^*$
	5.0217	246.90	0.0650	H-2 \rightarrow L+1 (+99%); H \rightarrow L (11%)	
	5.4719	226.59	0.0001	H-1 \rightarrow L+1 (+88%); H \rightarrow L+2 (+88%)	
	5.4759	226.42	0.0001	H-1 \rightarrow L+1 (+88%); H \rightarrow L+2 (+11%)	
	5.9466	208.50	0.0631	H-2 \rightarrow L (+11%); H \rightarrow L+1 (+85%)	
	6.0308	205.58	0.0019	H \rightarrow L+3 (+22%)	
P43HO	3.2274	384.16	0.0003	H \rightarrow L (+97%)	$\pi \rightarrow \pi^*$
	3.7565	330.06	0.0001	H \rightarrow L+1 (+2%)	
	4.4706	277.33	0.1436	H-2 \rightarrow L (+98.8%); H-1 \rightarrow L (+98%)	
	5.2709	235.22	0.0001	H \rightarrow L (+2%); H \rightarrow L+1 (+94%)	
	5.9533	208.26	0.0049	H-2 \rightarrow L+1 (+97%)	
	6.1255	202.41	0.0058	H \rightarrow L+2 (+97%); H \rightarrow L+4 (+2%)	
P4OL	5.0658	244.75	0.0000	H \rightarrow L (+99%)	$\pi \rightarrow \pi^*$
	5.2319	236.98	0.0045	H \rightarrow L+1 (+99%)	
	5.4179	228.84	0.0016	H-2 \rightarrow L+1 (+34%); H-1 \rightarrow L (+64%)	
	5.8038	213.63	0.0001	H-2 \rightarrow L+2 (+2%); H-1 \rightarrow L+2 (+95%);	
	6.0112	206.26	0.0040	H-2 \rightarrow L (+22%); ; H-1 \rightarrow L+1 (+52%); H \rightarrow L+2 (+23%)	
	6.0929	203.49	0.0140	H-2 \rightarrow L (+16%); H-1 \rightarrow L+1 (+8%); H \rightarrow L+2 (+72%)	
P21HO	4.3106	287.63	0.0966	H \rightarrow L (+97%)	$\pi \rightarrow \pi^*$
	4.4973	275.68	0.0001	H-1 \rightarrow L (+97%); H-1 \rightarrow L+2 (+3%)	
	5.0147	247.24	0.0017	H \rightarrow L+1 (+99%)	
	5.6233	220.48	0.0000	H-1 \rightarrow L+2 (+5%); H \rightarrow L+3 (+93%)	
	5.6423	219.74	0.0001	H-1 \rightarrow L (+2%); H-2 \rightarrow L+2 (+90%); H \rightarrow L+3 (+5%)	
	5.9010	210.11	0.0089	H \rightarrow L+4 (+98%)	
P2OL	5.0188	247.04	0.0034	H-1 \rightarrow L (+99%)	
	5.0658	244.75	0.0657	H-2 \rightarrow L+2 (+10%); H \rightarrow L (+88%)	
	5.5163	224.76	0.0001	H \rightarrow L+1 (+98%)	

Fig.5. The calculated UV spectra of 2-Pyridone and 2-Pyridinethione tautomers



3. 3. Polarizability and hyperpolarizability

The polarizabilities and hyperpolarizabilities characterize the response of a system in an applied electric field [10]. Theoretical calculation provides another method to investigate substantial characteristics of materials. The first order hyperpolarizability (β) of the title molecule is calculated using B3LYP 6-31++G (d,p) basis set based on the finite field approach. Theoretical studies have showed however, that this set supplemented by the addition of diffuse p and d functions, provides a considerable improvement on the estimates of the second hyperpolarizability of small organic molecular systems.[11-15] Hyperpolarizability is a third rank tensor that can be described by a 3X3X3 matrix. In presence of a static uniform electric field (F) the perturbed energy (E) of a molecule can be written as

$$E(F) = E_0 - \sum_i \mu_i F_i - \frac{1}{2!} \sum_{ij} \alpha_{ij} F_i F_j - \frac{1}{3!} \sum_{ijk} \beta_{ijk} F_i F_j F_k - \dots,$$

where E_0 is the energy of the molecule in the absence of an external electric field and μ_i are the components of the permanent dipole moment; α_{ij} are the components of the dipole polarizability; and β_{ijk} are the components of the first dipole hyperpolarizability. Here the average linear polarizability $\langle \alpha \rangle$ and the vector component of the first hyperpolarizability along the dipole moment direction β_{vec} [16, 17] are defined by the following equations:

$$\alpha = \frac{1}{3} (\alpha_{xx} + \alpha_{yy} + \alpha_{zz}) \quad (5)$$

The polarizability anisotropy invariant is

$$\Delta\alpha = \left[(\alpha_{xx} - \alpha_{yy})^2 + (\alpha_{yy} - \alpha_{zz})^2 + (\alpha_{zz} - \alpha_{xx})^2 \right]^{1/2} \quad (6)$$

Another quantity of interest is the total intrinsic quadratic hyperpolarizability given by

$$\beta = (\beta_x^2 + \beta_y^2 + \beta_z^2)^{1/2} \quad (7)$$

The complete equation for calculating the first-order hyperpolarizability from GAUSSIAN 09W output is given as follows:

$$\beta_{\text{tot}} = [(\beta_{\text{xxx}} + \beta_{\text{xyy}} + \beta_{\text{xzz}})^2 + (\beta_{\text{yyy}} + \beta_{\text{yzz}} + \beta_{\text{yxx}})^2 + (\beta_{\text{zzz}} + \beta_{\text{zxx}} + \beta_{\text{zyy}})^2]^{1/2}$$

(8)

Tables 2 and 3 list the values of the polarizabilities, anisotropy invariant and hyperpolarizabilities of the studied tautomers.

Polarizability increases with atomic or ionic radius; it depends on the effectiveness of nuclear screening and increases as each valence shell is filled. Table 3., gives the polarizability values for the 2-pyridone tautomers. Our β_{tot} results for the o-OH, the p-OH and the m-OH pyridines are, respectively, 51.99 esu, 52.98 esu and 55.35 esu. These results show that both o-nitro and p-OH substitutions changes the electron withdrawing ability of the nitro group, leading to a marked diminution of the β_{tot} values. The order of polarizability of 2- pyridine tautomers: P21HO > P3OL > P2OL > P4OL > P43HO > P34HO. The greater the polarizability of a molecule, the larger the induced dipole.

Table.3. The Polarizability(α)and Hyper polarizability(β)2-Pyridone and 2-Pyridinethione tautomers

Tauto Mer	$\langle\alpha\rangle$ a.u	(β) a.u	esu	$\Delta\alpha$ a.u
P34HO	51.99	18.90	1.5818×10^{-31}	1610.37
P3OL	54.57	20.03	1.6764×10^{-31}	1761.08
P43HO	52.98	10.25	0.8579×10^{-31}	1622.55
P4OL	53.88	40.78	3.4130×10^{-31}	1676.26
P21HO	55.35	27.70	2.3183×10^{-31}	2106.20
P2OL	54.43	24.21	2.0262×10^{-31}	1735.11

4. CONCLUSIONS

In this paper the antiradical activity, linear polarizability and first hyperpolarizability of of 2-pyridone tautomers are systematically investigated at the Density Functional theory (DFT) framework. In addition, the ground state geometries and electronic structures of six pyridine tautomers were investigated by TD-DFT method. From electrodonating (ω^-), electroaccepting (ω^+) power, donor R_d and acceptor R_a index, the order of good electron donors: P2OL < P21HO < P3OL < P34HO < P4OL < P43HO. The polarizability results show that both o-nitro and p-OH substitutions changes the electron withdrawing ability of the nitro group, leading to a marked diminution of the β_{tot} values. From the TD-DFT calculation, the first optically allowed electronic transition of λ_{max} for P34HO, P3OL, P43HO, P4OL, P21HO and P2OL are

predicted to populate the HOMO \rightarrow LUMO transitions at 310.66, 246.90, 277.33, 203.49, 287.63 and 244.75 nm, respectively.

REFERENCES

- [1] C. Lee, W. Yang, R. G. Parr, Phys. Rev. B 37 (1988) 785
- [2] Frisch MJ, Trucks GW, Schlegel HB et al. 2009. Gaussian 09, Rev. A.1 Gaussian, Inc Wallingford CT
- [3] M. K. Nazeeruddin, F. D. Angelis, S. Fantacci, A. Selloni, G. Viscardi, P. Liska, S. Ito, B. Takeru, M. Grätzel, J. Am. Chem. Soc. 127 (2005) 16835
- [4] A. Galano, J. Phys. Chem. B 111 (2007) 12898, <http://dx.doi.org/10.1021/jp074358u>.
- [5] J.L. Gazquez, A. Cedillo, A. Vela, J. Phys. Chem. A 111 (2007) 1966.
- [6] A. Martinez, M.A. Rodriguez-Girones, A. Barbosa, M. Costas, J. Phys. Chem. A 112 (2008) 9037,
- [7] M. Lappas, M. Permezel, J. Nutr. Biochem. 22 (2011) 1195.
- [8] J.P. Kamat, T.P.A. Devasagayam, Redox Rep. 4 (1999) 179.
- [9] D.M. Abdallah, Eur. J. Pharmacol. 627 (2010) 276.
- [10] C. R. Zhang, H. S. Chen, G. H. Wang, Chem. Res. Chin. U. 20 (2004) 640-646.
- [11] C. Adant, J.L. Bre ´das, and M. Dupuis, J. Phys. Chem. A 101, 3025,1997.
- [12] M. Yang, S. Li, J. Ma, and Y. Jiang, Chem. Phys. Lett. 354, 316,2002.
- [13] L.N. Oliveira, O.A.V. Amaral, M.A. Castro, and T.L. Fonseca, Chem. Phys. 289, 221 ,2003.
- [14] G.J.B. Hurst, M. Dupuis, and E. Clementi, J. Chem. Phys. 89, 385,1988.
- [15] C. Daniel and M. Dupuis, Chem. Phys. Lett. 171, 209 ,1990.
- [16] Y. Sun, X. Chen, L. Sun, X. Guo, W. Lu, Chem. Phys. Lett. 381 (2003) 397-403.
- [17] O. Christiansen, J. Gauss, J. F. Stanton, Chem. Phys. Lett. 305 (1999) 147-155.